THE JOURNAL OF BIOLOGICAL CHEMISTRY
Vol. 279, No. 43, Issue of October 22, pp. 44915–44923, 2004
Printed in U.S.A.


# Quantifying the Effects of Molecular Orientation and Length on Two-dimensional Receptor-Ligand Binding Kinetics*

Received for publication, June 23, 2004, and in revised form, August 3, 2004
Published, JBC Papers in Press, August 6, 2004, DOI 10.1074/jbc.M407039200

**Jun Huang‡§, Juan Chen‡, Scott E. Chesla¶, Tadayuki Yago‖, Padmaja Mehta‖, Rodger P. McEver‖**, Cheng Zhu§¶‡‡, and Mian Long‡§§**

*From the ‡National Microgravity Laboratory, Institute of Mechanics, Chinese Academy of Sciences, Beijing 100080, China, the ¶Woodruff School of Mechanical Engineering and §Coulter Department of Biomedical Engineering, Georgia Institute of Technology, Atlanta, Georgia 30332, and the ‖Cardiovascular Biology Research Program, Oklahoma Medical Research Foundation and **Department of Biochemistry and Molecular Biology and Oklahoma Center for Medical Glycobiology, University of Oklahoma Health Sciences Center, Oklahoma City, Oklahoma 73104*

**Surface presentation of adhesion receptors influences cell adhesion, although the mechanisms underlying these effects are not well understood. We used a micropipette adhesion frequency assay to quantify how the molecular orientation and length of adhesion receptors on the cell membrane affected two-dimensional kinetic rates of interactions with surface ligands. Interactions of P-selectin, E-selectin, and CD16A with their respective ligands or antibody were used to demonstrate such effects. Randomizing the orientation of the adhesion receptor or lowering its ligand- and antibody-binding domain above the cell membrane lowered two-dimensional affinities of the molecular interactions by reducing the forward rates but not the reverse rates. In contrast, the soluble antibody bound with similar three-dimensional affinities to cell-bound P-selectin constructs regardless of their orientation and length. These results demonstrate that the orientation and length of an adhesion receptor influences its rate of encountering and binding a surface ligand but does not subsequently affect the stability of binding.**

Cell adhesion is a fundamental biological process that is mediated by specific interactions between adhesion receptors and their ligands on other cell surfaces or in extracellular matrix (1, 2). For example, interactions between selectins and glycoconjugates mediate leukocyte tethering to and rolling on vascular surfaces at sites of inflammation or injury (3–5). The selectin family of adhesion molecules has three known members: P-, E-, and L-selectin. Their common structure is an N-terminal, C-type lectin (Lec)[1] domain, followed by an epidermal growth factor (EGF)-like module, multiple copies of consensus repeat (CR) units characteristic of complement binding proteins, a transmembrane segment, and a short cytoplasmic domain (3–5). As another example, circulating immunoglobulin G (IgG) binds to foreign particles or damaged tissue through their dual antigen-binding fragments (Fab). The conserved Fc fragment of this bifunctional molecule is available for binding by Fcγ receptors (FcγRs) on the immune cell surface. Such binding triggers a wide variety of immune responses (6).

To mediate cell adhesion, the interacting receptors and ligands must anchor apposing surfaces of two cells or of a cell and the substratum, *i.e.* two-dimensional binding, which differs from interactions in the fluid phase, *i.e.* three-dimensional binding. The binding affinity $K_a$ is the ratio of equilibrium concentration of bonds to those of free receptors and ligands. However, concentration is measured as number of molecules per volume in three dimensions but number of molecules per area (*i.e.* surface density) in two dimensions, resulting in different units for $K_a$ ($M^{-1}$ in three dimensions and $\mu m^2$ in two dimensions). The kinetic forward rate $k_f$ also has different units in different dimensions ($M^{-1}\ s^{-1}$ in three dimensions and $\mu m^2\ s^{-1}$ in two dimensions). The two-dimensional $k_f$ is the rate of bond formation between unit densities of receptors and ligands that are respectively anchored on two apposing surfaces of unit area. By comparison, the three-dimensional $k_f$ is the rate of bond formation between unit concentrations of receptors and ligands at least one of which is in solution of unit volume. There has been increasing recognition that two-dimensional binding parameters are not readily conversable from their three-dimensional counterparts (7). One of the reasons for this is that two-dimensional interactions are influenced by the surface environment, just as three-dimensional interactions are affected by the solvent environment (8). One of the surface environmental factors is the distance that the binding pocket of the adhesion receptor extends outward from the cell surface. For example, extending the binding site of CD58 above the cell membrane by interposing four Ig-like domains (~15 nm) in the stalk enhances its binding to CD2 on T lymphocytes (9). Under static conditions, P-selectin glycoprotein ligand 1 (PSGL-1)-expressing neutrophils adhere equivalently to cells expressing

* This work was supported by Natural Science Foundation of China Grants 10332060, 30225027, 10128205, and 10072071, Chinese Academy of Sciences Grant KJCX2-SW-L06, Ministry of Education grant TRAPOYT (to M. L.), and National Institutes of Health Grants AI 44902 and AI38282 (to C. Z.), TW 05774-01 (to C. Z. and M. L.), and HL 65631 (to R. P. M.). The costs of publication of this article were defrayed in part by the payment of page charges. This article must therefore be hereby marked "*advertisement*" in accordance with 18 U.S.C. Section 1734 solely to indicate this fact.

‡‡ To whom correspondence may be addressed: George W. Woodruff School of Mechanical Engineering and Wallace H. Coulter Department of Biomedical Engineering, Georgia Institute of Technology, Atlanta, GA 30332-0363. Tel.: 404-894-3269; Fax: 404-385-1397; E-mail: cheng.zhu@me.gatech.edu.

§§ To whom correspondence may be addressed: National Microgravity Laboratory, Institute of Mechanics, Chinese Academy of Sciences, Beijing 100080, P. R. China. Tel.: 86-10-6261-3540; Fax: 86-10-6261-3540; E-mail: mlong@imech.ac.cn.

[1] The abbreviations used are: Lec, lectin; EGF, epidermal growth factor; CR, consensus repeat; FcγRIIIA, Fcγ receptor IIIA or CD16A; PSGL-1, P-selectin glycoprotein ligand 1; RBC, red blood cell; $CrCl_3$, chromium chloride; FITC, fluorescein isothiocyanate; mIgG and RbIgG, mouse and rabbit IgG; sPs, P-selectin construct consisting of Lec-EGF domains plus nine CRs; PLE, P-selectin construct consisting of Lec-EGF domains; sEs, E-selectin construct consisting of Lec-EGF domains plus six CRs; ELE, E-selectin construct consisting of Lec-EGF domains; CHO, Chinese hamster ovary; mAb, monoclonal antibody.

wild-type P-selectin that contains 9 CR units and to P-selectin constructs with as few as two CRs. However, P-selectin requires at least 5 CRs to mediate optimal rolling of flowing neutrophils under dynamic shear conditions (10). K562 cells bearing 2-GSP-6, a glycosulfopeptide modeled after the binding domain of PSGL-1, which was attached to the membrane-distal region of a nonbinding molecule ~50 nm above the cell surface, roll more stably on P-selectin than cells bearing 2-GSP-6 randomly attached to cell surface proteins (11). HL-60 cells adhere to immobilized full-length E-selectin that contains all six CRs but not to shorter E-selectin constructs with two or less CRs (12).

Another surface environmental factor is the orientation of the binding pockets of adhesion receptors. For example, HL-60 cells adhere to the short E-selectin constructs with two or less CRs when they are captured by a nonblocking monoclonal antibody (mAb) adsorbed on the plastic surface (12). The ligand binding affinity and kinetics of FcγRIIIA (CD16A) are affected by its surface anchor (glycosylphosphatidylinositol or transmembrane) (13). Cell adhesion to fibronectin is modulated by surface chemistries that alter fibronectin adsorption (14). Cells expressing an L-selectin construct that replaces its EGF domain with the EGF domain of P-selectin roll better on L-selectin ligands than cells expressing wild-type L-selectin, perhaps because an altered orientation of the lectin domain enhances the association rate with surface ligands (15).

The differential effects of shortening P-selectin on adhesion under flow and static conditions (10) suggest that altering molecular length may affect the kinetics of the receptor-ligand interaction. The EGF domain swapping study (15) suggests that orientation also influences kinetics. To directly test this possibility, we quantified the effects of molecular orientation and length on cell adhesion by comparing the two-dimensional kinetics of the same molecules coupled to the surface of human red blood cells (RBCs) using different methods: coating via chromium chloride ($CrCl_3$) coupling, which led to random orientation, or capturing by a nonblocking mAb, which resulted in a more uniform orientation, or direct binding to the RBC surface via an anti-human RBC antibody, which yielded fully uniform orientation. Two-dimensional kinetics was also compared between captured short and long constructs of the same molecule. In addition, three-dimensional affinities and two-dimensional bindings of a mAb to surface-bound P-selectin constructs of different orientations and lengths were compared. Our results indicate that the orientation and length influence the two-dimensional forward rate but not the two-dimensional reverse rate of the molecular interaction, whereas they have no effects on three-dimensional affinity. These results provide insights into the biophysical mechanisms by which the molecular orientations and lengths of adhesion receptors affect cell adhesion.

## EXPERIMENTAL PROCEDURES

*Antibodies, Proteins, and Cells*—Anti-P-selectin blocking (G1) and capturing (S12) (16) monoclonal antibodies (mAbs), anti-E-selectin blocking (ES1) and capturing (ES3 and 1D6) mAbs (10, 17–18), and anti-PSGL-1 blocking mAb PL1 (19) (all mouse IgG1, mIgG1) have previously been described. Anti-CD58 mAb TS2/9 (mIgG1), anti-CD16A blocking mAb CLBFcgran-1 (mIgG2a) as well as the irrelevant control mAb X63 (mIgG1) were generous gifts from Dr. Periasamy Selvaraj (Emory University School of Medicine) (20). Fluorescein isothiocyanate (FITC)-labeled anti-P-selectin mAb G1 and anti-E-selectin mAb HAE-1f (mIgG1) were from Ancell Corporation (Bayport, MN). Rabbit anti-human RBC polyclonal antibody was from ICN/Valeant Pharmaceuticals International (Costa Mesa, CA). FITC-labeled goat anti-mouse and anti-rabbit polyclonal antibodies, irrelevant rabbit antibodies (RbIgG), and irrelevant control mIgG1 were from Sigma.

Soluble P-selectin (sPs) consisting of Lec-EGF domains plus nine CRs but no transmembrane and cytoplasmic domains (21) and soluble P-selectin (PLE) consisting of only the Lec-EGF domains with an added C-terminal epitope recognized by mAb 1478 (mIgG1) (22) have also been described. Soluble E-selectin (sEs) consisting of Lec-EGF domains plus six CRs but no transmembrane and cytoplasmic domains was obtained from R&D Systems Inc. (Minneapolis, MN). Soluble E-selectin (ELE) consisting of only the Lec-EGF domains was a generous gift from Dr. Kuo-Sen Huang of Hoffmann-La Roche Inc. (Nutley, NJ) (12).

Human promyelocytic leukemia HL-60 cells from ATCC were grown in RPMI 1640 media supplemented with 2 mM L-glutamine, 100 units/ml penicillin, 10 μg/ml streptomycin, and 10% fetal bovine serum. HL-60 cells constitutively express ligands for P- and E-selectin. Chinese hamster ovary (CHO) cells transfected to express human CD16A (from Dr. Periasamy Selvaraj) (20) were cultured in the same media plus 400 μg/ml geneticin (Invitrogen Life Technologies) as selection agent. The expression of CD16A was periodically checked via flow cytometry (FACSCalibur, BD Biosciences, San Jose, CA). The full IgG was cleaved into Fc fragment by Lampire (Pipersville, PA).

*Coupling Protein to RBCs*—A previously described modified chromium chloride method was used to couple capturing mAbs (S12, 1478, ES3, or 1D6), soluble selectin constructs (sPs, PLE, sEs, or ELE), anti-P-selectin mAb (G1), or irrelevant RbIgG onto the surface of fresh human RBCs (23–26). Coupling efficiency of proteins was examined by flow cytometry, using CD58 that is constitutively expressed on RBC at a known density as a standard (27). Selectin constructs and RbIgG so coated were randomly oriented (Fig. 1, *a*–*c*). To obtain a more uniform orientation, selectin constructs were captured on mAb-coated RBCs by incubation with 50–200 ng/ml of selectin constructs for 30 min at 4 °C before the micropipette experiment (Fig. 1, *a*, *b*, and *d*). To obtain fully uniform orientation of RbIgG for CD16A binding, RBCs were incubated with 10 ng/ml rabbit anti-human RBC polyclonal antibody for 30 min at 4 °C prior to the micropipette experiment (Fig. 1*c*).

*Site Density Determination*—Site densities of proteins coated on RBCs or expressed on CHO cells were measured using flow cytometry and/or immunoradiometric assay (IRMA). To measure densities of randomly oriented selectins coated via $CrCl_3$ coupling, RBCs were incubated with anti-selectin blocking mAbs (G1 or ES1) at a concentration of 10 μg/ml in 200 μl of FACS buffer (RPMI 1640, 5 mM EDTA, 1% bovine serum albumin, 0.02% sodium azide) on ice for 40 min, and then incubated with FITC-labeled goat anti-mouse secondary antibody. To measure densities of randomly or uniformly oriented RbIgG, RBCs were directly incubated with FITC-labeled goat anti-rabbit antibody. To measure CD16A expression, CHO cells were incubated first with anti-CD16 mAb CLBFcgran-1 and then with FITC-labeled goat anti-mouse secondary antibody. After washing, the cells were analyzed by flow cytometry. The site densities were then calculated by comparing the fluorescence intensities of the cells with those of standard beads (Bangs Labs, Fishers, IN) (24). To measure densities of uniformly oriented selectins (sPs, sEs, or PLE), one set of RBCs pre-coated with a range of densities of the relevant capturing mAb (five to seven densities for each selectin) were incubated with FITC-labeled goat anti-mouse antibody and the fluorescence intensities were measured using flow cytometry as above. Another set of RBCs precoated with the same range of densities of capturing mAb was incubated with the corresponding selectin and their site densities were measured by IRMA (21, 26, 28). A calibration curve was obtained for each selectin by plotting the selectin site density against the mean fluorescence intensity of the capturing mAb, thereby allowing calculation of the site densities of the uniformly oriented selectin from the mean fluorescence intensities of the capturing mAb.

*Two-dimensional Kinetics Measurements*—The micropipette adhesion frequency assay for measuring two-dimensional kinetics has previously been described (24–26). Briefly, a single selectin (or RbIgG)-coated RBC and a single carbohydrate ligand-expressing HL-60 cell (or a CD16A-expressing CHO cell) was, respectively, aspirated by two micropipettes with respective diameters of ~1.5 and ~3 μm via a suction pressure of 1–4 mm $H_2O$ (10–40 pN/μm$^2$). Adhesion between the RBC and the HL-60 (or CHO) cell was staged by placing them onto controlled contact via micromanipulation. The presence of adhesion at the end of a given contact period was detected mechanically by observing microscopically the deflection of the flexible RBC membrane upon retracting it away from the HL-60 (or CHO) cell. Such detection was reliable and unambiguous for >90% of the retractions, as clearly observable membrane deflections could be generated by a force as low as 2 pN at the RBC apex, far lower than the strength of a single bond (24, 25). This contact-retraction cycle was repeated a hundred times to estimate the adhesion probability, $P_a$, at that contact duration, $t$. For each surface presentation of each molecular species examined, ~100

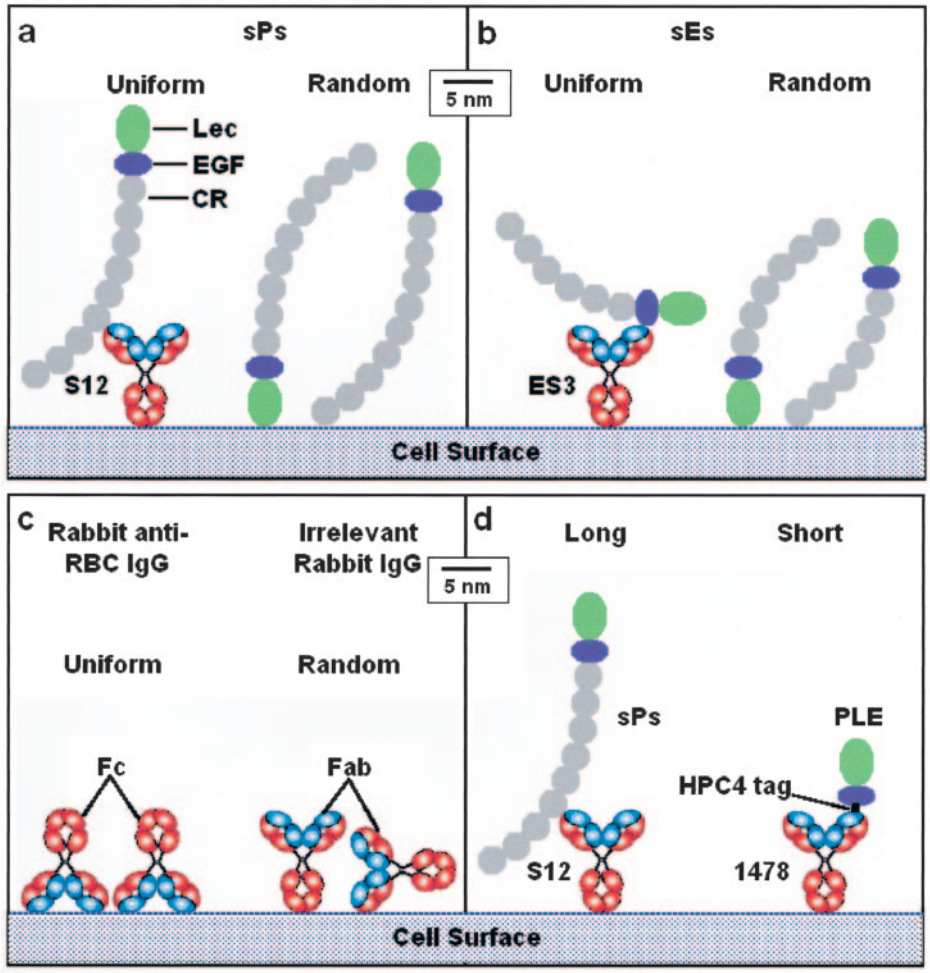


FIG. 1. **Schematics of long or short molecules coated on RBC surface with uniform or random orientation.** *a* and *b*, RBC surfaces coated with sPs or sEs with either uniform or random orientation. Uniform orientation was achieved by capturing sPs or sEs via its capturing mAb (S12 or ES3). Random orientation was obtained by directly coating sPs or sEs via $CrCl_3$ coupling. *c*, rabbit anti-human RBC IgG was oriented uniformly via binding to RBCs or irrelevant RbIgG was oriented randomly by coupling via $CrCl_3$. *d*, long sPs or short PLE was coated via their corresponding capturing mAbs (S12 or 1478), resulting in different extensions of the binding epitope above RBC surfaces.

pairs of cells were used to obtain several $P_a$ *versus* $t$ curves that correspond to different receptor and ligand densities, $m_r$ and $m_l$. Each binding curve was fitted to a small system probabilistic kinetic model (24–26) shown in Equation 1,

$$P_a = 1 - \exp\{-m_r m_l A_c K_a^0 [1 - \exp(-k_r^0 t)]\} \qquad \text{(Eq. 1)}$$

to estimate a pair of parameters: the zero force reverse rate, $k_r^0$, and effective binding affinity, $m_l A_c K_a^0$ (if $m_r$ was known) or $A_c K_a^0$ (if both $m_r$ and $m_l$ were known), where $A_c$ is the contact area, which was kept constant in all experiments. Multiple pairs of ($k_r^0$, $m_l A_c K_a^0$) or ($k_r^0$, $A_c K_a^0$) values were obtained for each molecular orientation and length to allow evaluation of the mean and S.D. The statistical significance of (or the lack thereof) the difference between the two-dimensional affinities (or reverse rates) of the same pair of interacting molecules being presented on the cell surface with different orientation or distance above the membrane was assessed using the Student's $t$ test.

In one set of experiments, adhesion frequencies between RBCs coated with G1 via $CrCl_3$ coupling and RBCs coated with P-selectin constructs of different orientations or lengths were measured at a single contact time of 4 s, and the results were expressed as $-\ln[1 - P_a]/(m_r m_l)$. 5–6 pairs of cells were measured for each P-selectin surface presentation, and the statistical significance of the differences between results from different conditions were assessed by the Student's $t$ test.

*Three-dimensional Affinity Measurements*—Scatchard analysis was used to determine three-dimensional binding affinities of $^{125}$I-labeled G1 in fluid phase for either long (sPs) or short (PLE) P-selectin constructs coated on RBC surfaces either uniformly by capturing mAbs (S12 or 1478) precoated via $CrCl_3$ coupling or randomly via direct $CrCl_3$ coupling (29, 21). Briefly, 200 $\mu$l of 0.1–6 $\mu$g/ml $^{125}$I-G1 was added to $5 \times 10^6$ P-selectin-coated RBCs. After incubation at 4 °C for 30 min, 500 $\mu$l of a 1:9 ratio of apiezon oil:dibutyl phthalate (Sigma) oil mixture was added into each sample, which was then centrifuged to separate the free $^{125}$I-labeled G1 from the cells. Radioactivity associated with the cell pellets was measured using a gamma counter. Specific binding of G1 was calculated by subtracting the nonspecific binding, which was determined by adding 50 times excess unlabeled G1, from total binding. All assays were performed in triplicate. The statistical significance of the difference between three-dimensional affinities for different molecular orientations or lengths was performed using the Student's $t$ test.

## RESULTS

*Binding Is Specific*—Binding was quantified by the adhesion frequency at sufficiently long contact time ($t \to \infty$) in control experiments. As exemplified for binding of P-selectin-coated RBCs to PSGL-1-expressing HL-60 cells (Fig. 2), adhesion frequencies measured from the micropipette assay were mediated by specific selectin-ligand interactions, because they were present when the RBCs were coated with appropriate nonblocking anti-selectin mAbs to capture the corresponding soluble selectin constructs but were abolished when mismatched selectin constructs not recognized by the coated capturing mAbs or isotype-matched irrelevant mAbs were used (Fig. 2). In addition, binding was blocked by mAbs against PSGL-1 (PL1), P-selectin (G1), and by the calcium chelator EDTA. Binding specificity between P-selectin-coated RBCs and G1-coated RBCs, E-selectin-coated RBCs and HL-60 cells, and between RbIgG-coated RBCs and CD16A-expressing CHO cells were confirmed by similar experiments (data not shown).

*Binding Curves Follow Simple Receptor-ligand Binding Kinetics*—Dependence of adhesion frequency on contact duration was measured using the micropipette assay at contact times ranging from 0.25–10 s, as exemplified for P-selectin-coated RBCs interacting with HL-60 cells (Figs. 3, *a* and *b*; 6, *a* and *b*). The adhesion probability, $P_a$, was obtained by removing the nonspecific adhesion frequency, $P_n$ (*dashed lines* in Figs. 3, *a* and *b*; 6, *a* and *b*, obtained by fitting the directly measured

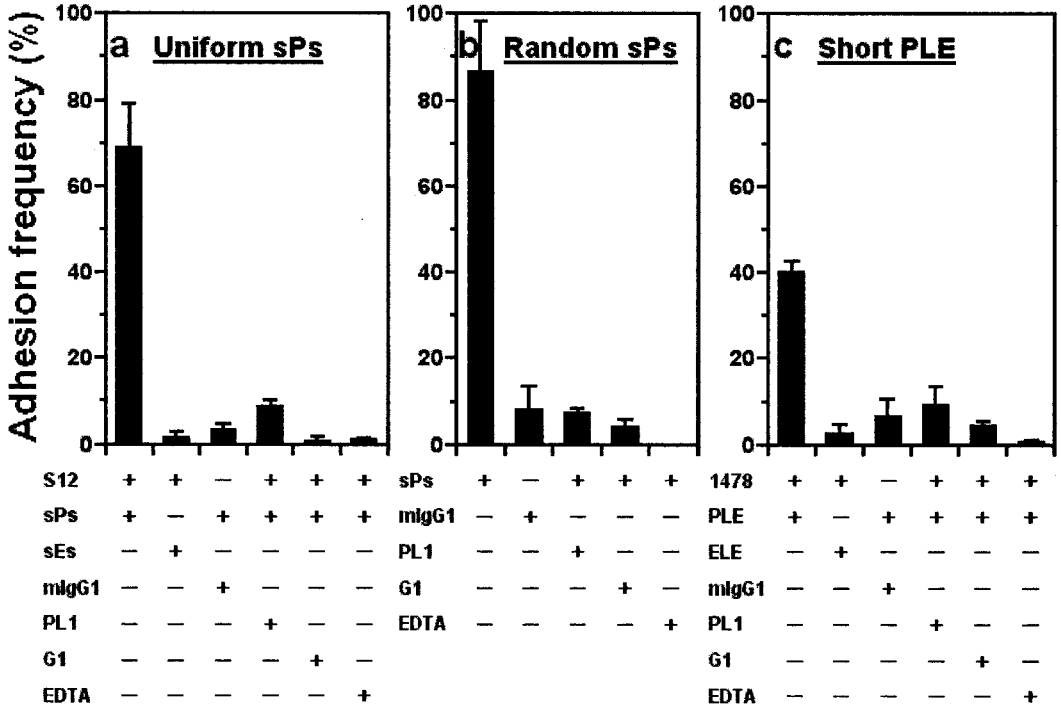


FIG. 2. **Binding specificity of P-selectin.** RBCs coated with sPs via capturing mAb S12 (*a*) or via direct $CrCl_3$ coupling (*b*) or with PLE via capturing mAb 1478 (*c*) adhered with high frequencies to PSGL-1-expressing HL-60 cells. Binding was abolished when the P-selectin construct (sPs or PLE) was substituted by an irrelevant E-selectin construct (sEs or ELE) that did not interact with the coated capturing mAbs or when the capturing mAb (S12 or 1478) was replaced by an irrelevant mIgG1. Adhesions were also blocked by the anti-PSGL-1 blocking mAb PL1, by the anti-P-selectin blocking mAb G1, and by the calcium chelator EDTA. Adhesion frequency for each condition was obtained by fitting the $P_a$ *versus* $t$ curves to Equation 1 and then setting $t \rightarrow \infty$, where the curves were obtained from 4~36 cell pairs with 100 contacts each cell pair. Data are presented as the mean ± S.E.

nonspecific adhesion frequency to Eq. 1), from the directly measured total adhesion frequency, $P_t$, according to $P_a = (P_t - P_n)/(1 - P_n)$ (30). The data (*points* in Figs. 3, *a* and *b*; 6, *a* and *b*) exhibit the shape of typical binding curves, with a transient phase where $P_a$ increased with $t$ and a steady phase where $P_a$ reached equilibrium. Equation 1 was used to fit each binding curve to obtain two parameters: $k_r^0$ and $m_l A_c K_a^0$ (if $m_r$ was known) or $k_r^0$ and $A_c K_a^0$ (if both $m_r$ and $m_l$ were known). For each set of interacting molecules presented on the RBC surface at each orientation and length, the mean reverse rate and mean effective binding affinity were calculated from several pairs of $k_r^0$ and $m_l A_c K_a^0$ (or $A_c K_a^0$) values that respectively best fitted several $P_a$ *versus* $t$ curves obtained by varying the densities of the receptors and/or ligands. The mean $k_r^0$ and $m_l A_c K_a^0$ (or $A_c K_a^0$) values were then used, along with the corresponding $m_r$ and/or $m_l$ values measured from independent experiments, to predict each $P_a$ *versus* $t$ curve (*solid lines* in Figs. 3, *a* and *b*; 6, *a* and *b*). It is evident that the model fits the data well, imparting confidence in the estimated kinetic parameters.

*Molecular Orientation Affects Forward Rates but Not Reverse Rates*—To alter molecular orientation, soluble selectin constructs were coated randomly via $CrCl_3$ or coupled more uniformly via capturing by a mAb precoated on RBC surfaces (see Fig. 1, *a* and *b*). For each coating method, densities of selectin binding sites were quantified using adhesion blocking mAbs, and $P_a$ *versus* $t$ curves were measured using the micropipette assay. To bind HL-60 cells with the same level of steady-state adhesion frequency, ~3.5-fold higher site density was required for RBCs coupled with randomly oriented sPs than for RBCs coupled with uniformly oriented sPs (*e.g.* compare curves labeled 2.4 $\mu m^{-2}$ in Fig. 3*a* and 8.7 $\mu m^{-2}$ in Fig. 3*b*). By comparison, the time required to reach half equilibrium binding level, $t_{1/2}$, was indifferent to the coating methods. Since the equilibrium binding $P_a(\infty)$ is related to the effective binding affinity, $m_l A_c K_a^0 = -\ln[1 - P_a(\infty)]/m_r$ (if $m_r$ was known) or $A_c K_a^0 = -\ln[1 - P_a(\infty)]/(m_r m_l)$ (if $m_r$ and $m_l$ were known), and the half-time $t_{1/2}$ is related to the reverse rate, $k_r^0 \approx 0.5/t_{1/2}$ (13, 24), our data indicate that, when both interacting molecules were immobilized on cell surfaces, randomly oriented sPs bound ligands with a lower effective binding affinity but a similar reverse rate compared with the more uniformly oriented sPs. These observations were confirmed by comparing the kinetic parameters obtained from fitting Equation 1 to the $P_a$ *versus* $t$ curves (Fig. 3*c*). The zero force reverse rates for the randomly oriented and more uniformly oriented sPs were similar ($k_r^0 = 1.1 \pm 0.1$ and $0.9 \pm 0.1$ $s^{-1}$, respectively, $p > 0.45$). By contrast, the effective affinity for the randomly oriented sPs was 3.1-fold lower than that for the more uniformly oriented sPs ($m_l A_c K_a^0 = 0.08 \pm 0.002$ and $0.25 \pm 0.01$ $\mu m^2$, respectively, $p < 0.015$). The effective forward rate (calculated from $m_l A_c k_f^0 = m_l A_c K_a^0 \times k_r^0$) for the randomly oriented sPs was 2.6-fold lower than that for the more uniformly oriented sPs ($m_l A_c k_f^0 = 0.09$ and $0.23$ $\mu m^2/s$, respectively). This isolation of the orientation effects to the forward rate suggests that better receptor orientation on the cell surface enhances effectiveness for ligand binding by providing easier access to ligands immobilized on the apposing cell surface. It follows from this hypothesis that the dissociation of preformed receptor-ligand bond would not be affected by orientation, as was observed.

The above hypothesis was further tested using E-selectin, a molecule structurally related to P-selectin. sEs was coated to the RBC surfaces either randomly via $CrCl_3$ coupling or more uniformly by a capturing mAb (ES3) precoated via $CrCl_3$ coupling. Here, ~8-fold higher site density was required for RBCs coated with randomly oriented sEs than that required for RBCs coated with more uniformly oriented sEs to bind HL-60 cells with the same level of steady-state adhesion frequency (data not shown). This translates to a 6.0-fold lower effective affinity

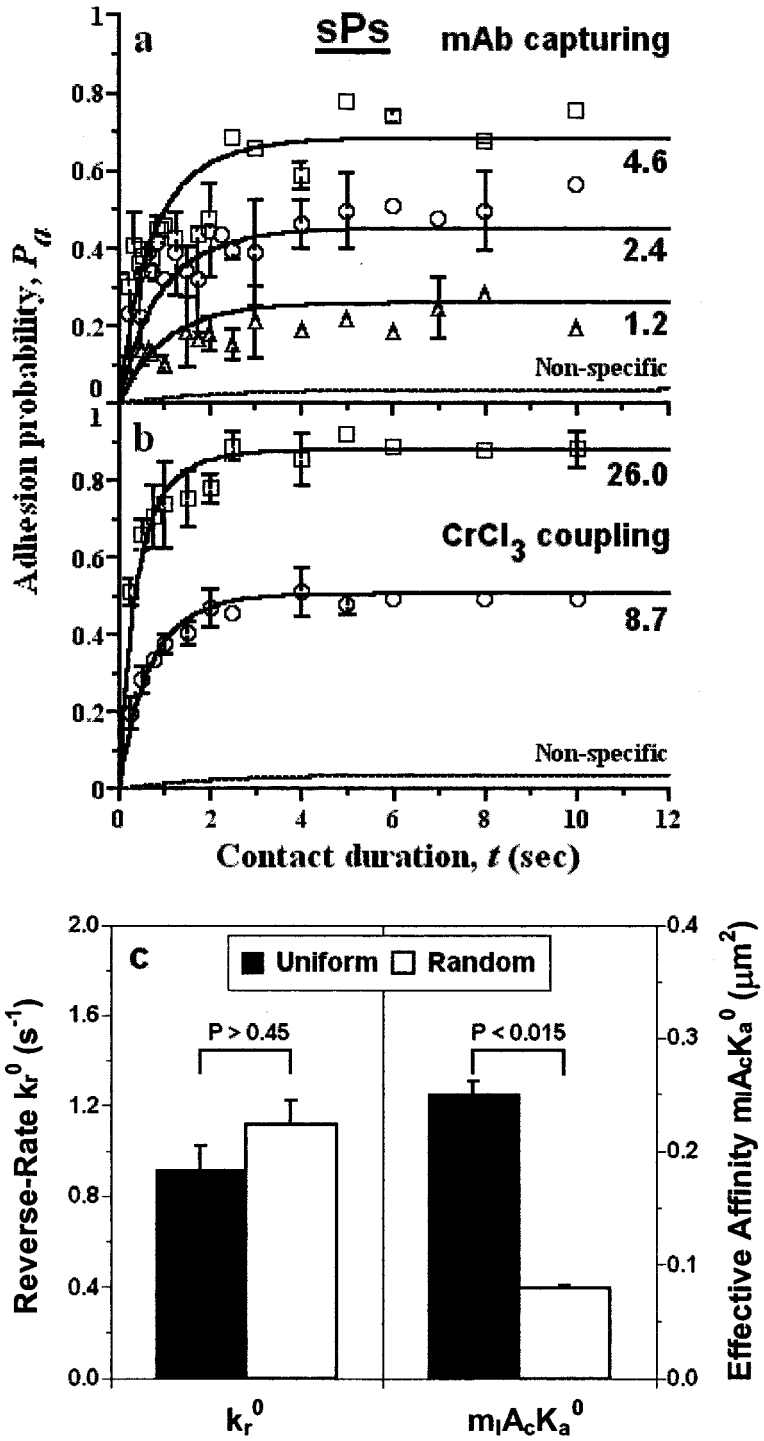


FIG. 3. **Binding curves and kinetics of uniformly or randomly oriented sPs.** Adhesion probability was plotted against contact duration at different site densities of $m_r$ = 4.6, 2.4, and 1.2 $\mu m^{-2}$ for uniformly oriented sPs (*a*), and 26 and 8.7 $\mu m^{-2}$ for randomly oriented sPs (*b*), respectively. Experimental data (*points*), presented as the mean ± S.E. at each contact time and obtained from 27–33 cell pairs for each curve, were compared with the predictions (*solid lines*) calculated from Equation 1 using the averaged best-fit kinetic parameters and the corresponding $m_r$ values. The *dashed line* represents nonspecific binding, obtained by fitting Equation 1 to the nonspecific data (23 and 28 data points in *a* and *b*, respectively, not shown for the sake of clarity). Mean ± S.D. of reverse rates, $k_r^0$, and effective binding affinities per unit site density of P-selectin, $m_l A_c K_a^0$, of uniformly (*solid bars*) and randomly (*open bars*) oriented sPs interacting with PSGL-1 are presented in *c*. *p* value indicates the level of statistical significance of differences in parameters corresponding to the two orientations.

for the randomly oriented than the more uniformly oriented sEs ($m_l A_c K_a^0$ = 0.002 ± 0.00008 and 0.012 ± 0.002 $\mu m^2$, respectively, $p < 0.08$) (Fig. 4). By comparison, the zero force reverse rates for the randomly and more uniformly oriented sEs were similar ($k_r^0$ = 0.9 ± 0.1 and 0.9 ± 0.5 $s^{-1}$, respectively, $p > 0.8$). The calculated effective forward rate for randomly oriented sEs was 5.0-fold lower than that for more uniformly oriented sEs ($m_l A_c k_f^0$ = 0.002 and 0.010 $\mu m^2/s$, respectively). These data support the validity of our hypothesis regarding mechanism of the orientation effect.

Additional test of our hypothesis was done using the CD16A-RbIgG interactions, a molecular system very different from the selectins. Uniformly oriented coating was achieved by using an anti-human RBC RbIgG, which bound the RBC surface via the two Fab binding sites, thereby orienting the constant Fc domain outward for CD16A binding. Randomly oriented coating was achieved by using $CrCl_3$ coupling of an irrelevant RbIgG. Two $P_a$ *versus* $t$ curves with different $m_r$ and $m_l$ levels were measured for each RbIgG orientation, and the corresponding kinetic parameters were evaluated by fitting Equation 1 to the data. As shown in Fig. 5, the effective affinity for the randomly oriented RbIgG was 5.2-fold lower than that for the uniformly oriented RbIgG ($A_c K_a^0$ = (0.29 ± 0.03) × $10^{-5}$ and (1.52 ± 0.26) × $10^{-5}$ $\mu m^4$, respectively, $p < 0.015$), while zero force reverse rates were similar ($k_r^0$ = 0.15 ± 0.04 and 0.24 ± 0.11 $s^{-1}$, respectively, $p > 0.45$). The effective forward rate for the

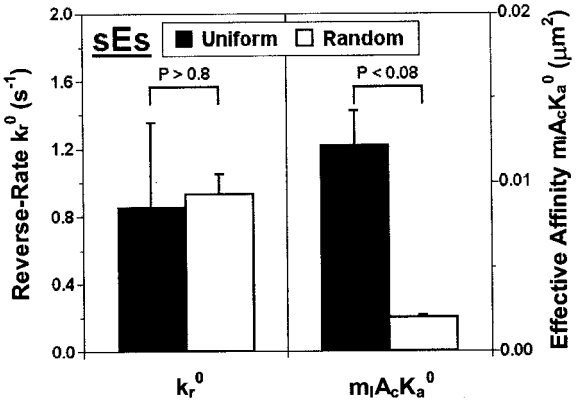


FIG. 4. **Kinetics of uniformly or randomly oriented sEs.** Micropipette experiments were performed using sEs respectively coated uniformly (two curves, $m_r$ = 37 and 12 $\mu m^{-2}$) or randomly (three curves, $m_r$ = 540, 290, and 130 $\mu m^{-2}$). 13–19 pairs of RBC-HL-60 cells were measured for each binding curve. The reverse rates, $k_r^0$, and effective binding affinities per unit site density of E-selectin, $m_l A_c K_a^0$, for carbohydrate ligands on HL-60 cells interacting with sEs coated on RBCs with uniform (*solid bars*) and random (*open bars*) orientation were obtained by fitting Equation 1 to the data and presented as mean ± S.D. $p$ value indicates the level of statistical significance of differences in parameters corresponding to the two orientations.

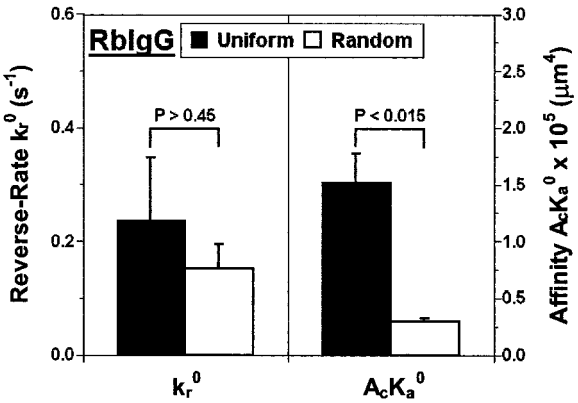


FIG. 5. **Two-dimensional kinetic reverse rates and effective affinities of CD16A for uniformly or randomly oriented RbIgG.** Adhesion experiments were performed using two sets of receptor and ligand densities for each orientation: $m_r \times m_l$ = 1200 × 40 and 240 × 40 $\mu m^{-4}$ for uniformly captured RbIgG and 240 × 190 and 1200 × 360 $\mu m^{-4}$ for randomly coupled RbIgG, respectively. The reverse rates, $k_r^0$, and effective binding affinities, $A_c K_a^0$, for CHO cell CD16A interacting with uniformly (*solid bars*) and randomly (*open bars*) oriented RbIgG were obtained by fitting Equation 1 to the data and presented as mean ± S.D. $p$ value indicates the level of statistical significance of differences in parameters corresponding to the two orientations.

randomly oriented RbIgG was 8.3-fold lower than that for the uniformly oriented RbIgG ($A_c k_f^0$ = 0.44 × $10^{-6}$ and 3.65 × $10^{-6}$ $\mu m^4$/s, respectively). These data corroborate the previous results and provide additional support to the conclusion that uniformly oriented molecules bind their countermolecules with higher effective affinity than randomly oriented molecules.

*Molecular Length Affects Forward Rates but Not Reverse Rates*—Previous flow chamber experiment has shown that more neutrophils accumulated on a long sPs than on a short PLE coated on the chamber floor at matched densities, demonstrating the effects of length on transient adhesion (22). To quantify the effects of molecular length on two-dimensional ligand binding kinetics, micropipette experiments were performed using the same P-selectin constructs: sPs was captured by mAb S12, which binds the 4th CR from the membrane anchor (10), whereas PLE was captured by mAb 1478, which binds an epitope tag added to the C terminus of the EGF domain. Thus, both P-selectin constructs were oriented properly on their respective RBC surfaces but the sPs extends the lectin binding pocket 5 CRs, or 15 nm, further outward from the RBC surfaces than the PLE (Fig. 1*d*). For nearly identical site densities (4.6 and 4.8 $\mu m^{-2}$, respectively), the steady-state adhesion frequencies were higher for the long sPs than the short PLE (0.68 and 0.42, respectively) (Fig. 6, *a* and *b*). By comparison, the time required to reach half steady-state level was similar for the two P-selectin constructs of different lengths. These observations were confirmed by comparing the kinetic parameters obtained from fitting Equation 1 to the $P_a$ *versus* $t$ curves (Fig. 6*c*). The effective affinity for the long sPs was 2.3-fold higher than that for the short PLE ($m_l A_c K_a^0$ = 0.25 ± 0.01 and 0.11 ± 0.003 $\mu m^2$, respectively, $p < 0.03$), while the zero force reverse rates were similar for the long and short constructs ($k_r^0$ = 0.9 ± 0.1 and 1.1 ± 0.1 $s^{-1}$, respectively, $p > 0.4$). The effective forward rate for long sPs was 1.9-fold higher than that for short PLE ($m_l A_c k_f^0$ = 0.23 and 0.12 $\mu m^2$/s, respectively). The similarity in the effects of molecular length and orientation on the two-dimensional forward rates but not the reverse rates suggests a similar underlying mechanism: sPs is more effective to bind ligands than PLE because it is easier for surface-bound ligands to access long than short receptors anchored on the apposing cell surfaces; however, the dissociation of preformed receptor-ligand bond would not be affected by the molecular length.

*Lack of Effects of Molecular Orientation and Length on Three-dimensional Affinity*—The isolation of the effects of molecular orientation and length to the forward rate suggests that randomizing the orientation and shortening the length of a membrane-bound molecule reduce its accessibility by the binding partner, especially when the partner is also anchored to the apposing cell membrane that restricts its ability to bind a molecule with suboptimal orientation and length. This hypothesis predicts that the effects of molecular orientation and length are associated primarily with two-dimensional binding, and will diminish if the countermolecules are no longer restricted by their surface anchor. Supporting this prediction, fluid phase sPs and PLE bind to immobilized PSGL-1 with similar three-dimensional binding affinities (3.1 × $10^6$ $M^{-1}$), as measured by surface plasmon resonance (31). To further test this prediction we compared the solution affinities of long sPs or short PLE coated on RBCs randomly via $CrCl_3$ coupling or more uniformly by a capturing mAb (S12 or 1478) pre-coated via $CrCl_3$ coupling. Because sufficient soluble PSGL-1 was unavailable, the three-dimensional affinities were measured using a $^{125}$I-labeled anti-P-selectin blocking mAb (G1) by Scatchard plot analysis (29, 21) (Fig. 7*a*). The three-dimensional affinities obtained from the negative slope of the linear fit to the Scatchard plot (correlation coefficients $R^2 > 0.97$ for all data) were similar for all four combinations of long or short P-selectin randomly or uniformly coated (Fig. 7*b*; $p > 0.1$~0.4). These results support our prediction and suggest that deletion of the consensus repeats and $CrCl_3$ coupling did not alter the conformation of the ligand binding region.

To further confirm our prediction regarding the effects of molecular orientation and length on two-dimensional (but not on three-dimensional) affinity and kinetics, micropipette experiments were performed to measure adhesion probabilities at $t_0$ = 4 s of the same anti-P-selectin mAb (G1, coated on RBC via $CrCl_3$ coupling) to the same RBCs used in the above three-dimensional affinity experiment, which were coated with short or long P-selectin with random or more uniform orientation. The results were expressed as $y = -\ln[1 - P_a(t_0)]/(m_r m_l) = A_c K_a^0 [1 - \exp(-k_r^0 t_0)]$ according to Equation 1 (Fig. 7*c*). Although the reverse rate $k_r^0$ could not be determined from meas-

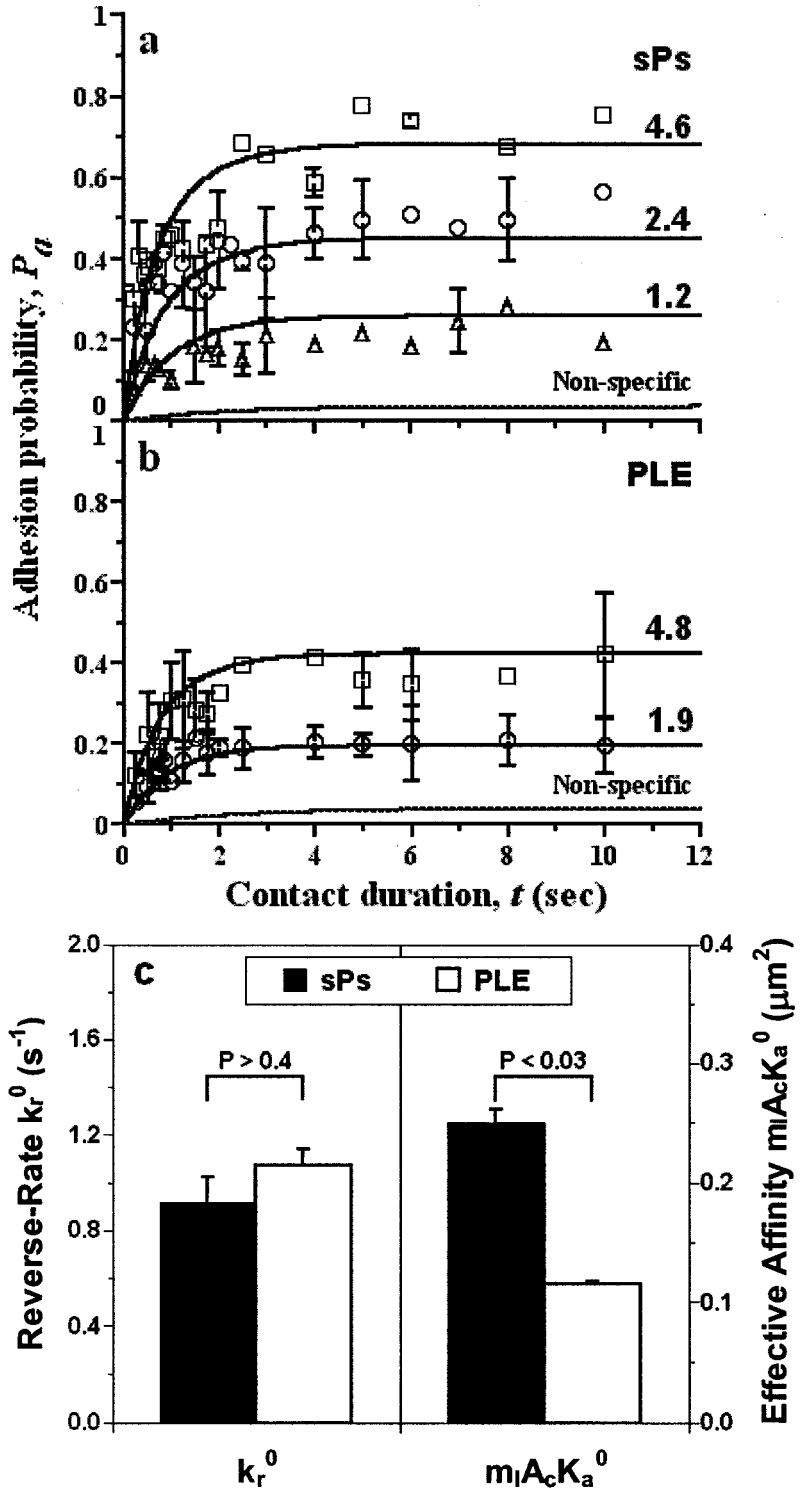


FIG. 6. **Binding curves and kinetics of long or short P-selectin constructs.** Adhesion probability was plotted against contact duration for different site densities: $m_r$ = 4.6, 2.4, and 1.2 $\mu m^{-2}$ for sPs (*a*), and 4.8 and 1.9 $\mu m^{-2}$ for PLE (*b*), respectively. Experimental data (*points*), obtained from 27~40 cell pairs each curve and presented as the mean ± S.E. at each contact time, were compared with the predictions (*solid lines*), obtained by fitting Equation 1 to the data. The *dashed line* represents nonspecific binding, obtained by fitting Equation 1 to the nonspecific data. Mean ± S.D. of reverse rates, $k_r^0$, and effective binding affinities per unit site density of P-selectin, $m_rA_cK_a^0$, of long sPs (*solid bars*) and short PLE (*open bars*) interacting with PSGL-1 were presented in *c*. *p* value indicates the level of statistical significance of differences in parameters corresponding to the two lengths.

urement at a single time point, the data in Figs. 3–6 indicate that it should be indifferent to the molecular orientation and length. Thus, the differences in the measured $-\ln[1 - P_a(t_0)]/(m_rm_l)$ values most likely reflect different two-dimensional affinities, or more precisely, different forward rates. As expected, strong orientation and length effects were clearly observable (Fig. 7*c*). The qualitatively similar effects of the molecular orientation and length observed in very different molecular systems, selectin-ligand, FcγR-IgG Fc, and antibody-antigen interactions, indicate the biophysical rather than biological basis of such effects, which do not depend on whether the molecules (selectin ligand, FcγR, or G1) are naturally expressed on the nucleated cell surface or artificially coated on the RBC surface with $CrCl_3$ coupling.

*Uniform Orientation and Extended Length Cooperatively Enhance Two-dimensional Binding Affinity*—We have shown that two aspects of surface presentation of adhesive molecules, their orientation and length, affected their two-dimensional binding affinity and kinetics. The isolation of such effects to the forward rate suggests a common biophysical mechanism. This mechanism predicts that the adverse effects of randomizing the orientation and shortening the length of the molecule can be compounded when short molecules are randomly oriented on cell surface. This hypothesis is supported by the data in Fig. 7*c*,

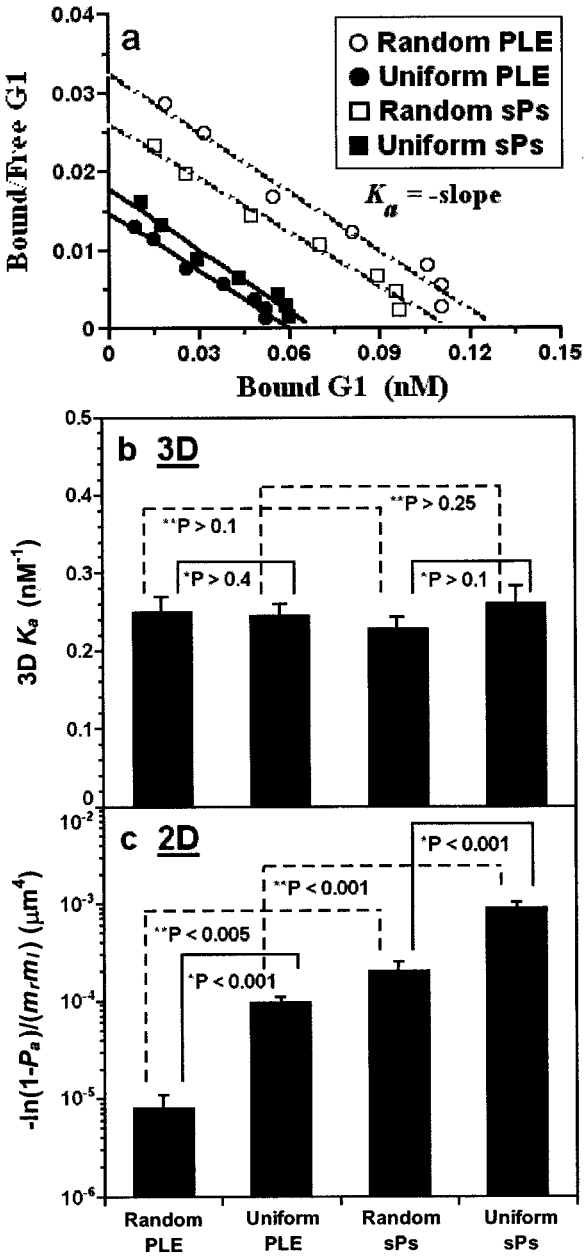


FIG. 7. **Three-dimensional affinity and two-dimensional binding of G1 to P-selectin constructs.** *a*, Scatchard plot analysis for three-dimensional affinity of $^{125}$I-labeled mAb G1 in fluid phase for long or short P-selectin construct coated on RBCs with either uniform or random orientation: uniformly oriented sPs (*solid squares* and *solid line*), uniformly oriented PLE (*solid circles* and *solid line*), randomly oriented sPs (*open squares* and *dotted line*), and randomly oriented PLE (*open circles* and *dotted line*). *b*, three-dimensional binding affinities were presented as mean ± S.D. for comparison with different orientations (*) or length (**). *c*, two-dimensional binding of G1-coated RBC to P-selectin-coated RBCs measured by micropipette at 4 s contact time. Data were presented as mean ± S.E. for comparison with different orientations (*) or length (**). *p* value indicates the level of statistical significance of differences in parameters for the two different orientations or lengths.

where the reduction in binding due to randomizing the molecular orientation is greater for the short PLE than for the long sPs (25- *versus* 9.2-fold). Alternatively, the reduction in binding caused by shortening the molecular length is greater for the randomly oriented than for the more uniformly oriented molecules (12- *versus* 4.3-fold). Thus, the cooperative effect of orientation and length amounts to a total of ~110-fold reduction in effective two-dimensional affinity for surface bound G1 from the more uniformly oriented long sPs to the randomly oriented short PLE. This is remarkable in view of their comparable three-dimensional affinities for the solution G1 (Fig. 7*b*). Similarly striking cooperative effects were also observed in micropipette experiments using RBCs coated with randomly oriented short molecules, PLE, ELE, or Fc fragment of IgG interacting with HL-60 cells or CD16A-expressing CHO cells. Despite the high molecular densities as assessed by flow cytometry, adhesion frequencies remained comparable to nonspecific adhesions, thereby preventing kinetic rates from being measured (data not shown). By comparison, much higher adhesion frequencies were detected using similar site densities of the same short but more uniformly oriented molecules (PLE and ELE, captured by mAbs 1478 and 1D6, respectively) (Fig. 6 and Ref. 26) or of their long but randomly oriented counterpart molecules (sPs, sEs, and RbIgG) (Figs. 3–6), thereby allowing kinetic measurements. These combined data demonstrate that uniform orientation and extended length cooperatively enhance two-dimensional binding affinity.

## DISCUSSION

The mechanisms by which differential orientations of cell adhesion receptors affect their functions are not well understood. The goal of the present study was to quantify such effects in terms of the two-dimensional kinetics of receptor-ligand binding. In addition, kinetic and affinity measurements in both two-dimension and three-dimension were used to elucidate the biophysical bases of such effects. One type of alteration in the molecular presentation on the RBC surface was achieved by coating the same molecule via either direct $CrCl_3$ coupling, antibody capturing, or anti-RBC binding (Fig. 1, *a*--*c*). Another type of alteration was achieved by shortening the length of the molecule by deleting part of its non-binding stalk (Fig. 1*d*). Both types of alterations were found to reduce the two-dimensional forward rate but not the reverse rate (Figs. 3–6). In addition, neither type of alterations seemed to affect the three-dimensional binding affinity (Fig. 7, *a* and *b*).

Cell adhesion assays require presentation of adhesion molecules on cell membranes or artificial surfaces. It has long been noticed that different methods of functionalizing the surface with adhesion molecules result in differential cell adhesion. Such effects could be due to changes in molecular orientation or conformation. For example, the surface anchor (glycosylphosphatidylinositol *versus* transmembrane) of CD16A influences its ligand binding kinetics and affinity (13), which has been attributed to conformational differences. This is because the same effects were observed in both two-dimensional and three-dimensional binding and for both receptor-ligand interactions and antibody-antigen interactions. Furthermore, the effects were ligand- and antibody-specific, because the effects were inverted when a different ligand or antibody was used (13). Another example is that NIH 3T3 fibroblasts adhered better to fibronectin absorbed on OH-group expressing self-assembled monolayers than to fibronectin absorbed on COOH-, $NH_2$- or $CH_3$-group expressing monolayers. This effect was interpreted as substrate-dependent conformational changes in fibronectin, since differential binding was also observed for soluble anti-fibronectin mAb and for cell surface $\alpha_5\beta_1$ integrin (32).

Our results indicate that altering the molecular orientations and lengths of adhesion receptors can affect their functions without altering the conformation of the ligand binding domain. This conclusion is supported by multiple lines of evidence. Conformational changes of the binding site likely affect reverse rate while orientation changes of the binding site likely affect forward rate (33). Extending the binding site above the surface by adding a polymer chain spacer can generate a long range attractive force that may enhance the forward rate but

would not affect the reverse rate (34). Randomizing orientation would reduce accessibility, thereby affecting forward rate, but would have little effect on the stability of the bond once it is formed, thereby not affecting reverse rate. These were exactly what were observed (Figs. 3–5).

The fact that similar effects were observed for four molecular systems, two of which are structurally related (P-selectin and E-selectin) but the other two not (RbIgG and G1), also suggests that the different coating methods caused changes in orientation rather than in conformation. Like physiosorption, $CrCl_3$ coupling likely results in random orientation that renders some of the immobilized molecules inaccessible for binding by the counter molecules. Coating with an anti-RBC antibody results in uniform orientation of the Fc portion of IgG for Fc$\gamma$R binding that is identical to the physiological situations. Capturing the molecules via nonblocking mAbs results in an intermediate degree of uniformity in orientation as the capturing mAbs themselves were randomly coated on RBC via $CrCl_3$ coupling. Consistent with this contention, the forward rate changes produced by different coating methods were greater for the Fc$\gamma$R system than the two selectin systems (compare Figs. 3*c* and 4 with Fig. 5).

It follows from the above arguments that shortening the molecular length would produce similar effects, as this likewise would affect accessibility but not stability, which was also observed (Fig. 6). Furthermore, the same reasoning predicts that the effects of random orientation would be worse by shortening the molecule; or conversely, that the diminishing binding due to random orientation could be partially restored by lengthening the molecule. Indeed, for similar differences in the degree of uniformity, the effects for the shorter E-selectin seemed greater than for the longer P-selectin (compare Figs. 3*c* and 4) and the effects for the even shorter G1 seemed the greatest (Fig. 7*c*). In addition, while randomizing the orientation of the long molecules (sPs, sEs, and RbIgG) via $CrCl_3$ coupling reduced binding, doing the same using their short counterparts (PLE, ELE, and Fc fragment of IgG) diminished binding below the level detectable by our micropipette assay (data not shown).

Finally, it seems intuitive that altering molecular orientation and length would affect two-dimensional binding but not three-dimensional binding. The reason is that two-dimensional binding places far greater demands on accessibility due to the linkage of the molecules to apposing surfaces, which restricts their motions in two-dimensional. Releasing one of the molecules from the surface enables it to approach its binding partner via three-dimensional motions, which likely allows it to gain access to suboptimally oriented and shortened molecules that are inaccessible to its surface-bound counterpart. Indeed, Scatchard plot analysis showed similar three-dimensional affinities of an anti-P-selectin mAb for P-selectin regardless of its orientation and length (Fig. 7), thereby supporting the above reasoning and indicating the lack of conformational changes near the P-selectin ligand binding site. Additionally, biosensor experiment has shown similar three-dimensional binding affinities of PSGL-1 for sPs and PLE (31).

Thus, the present work provides not only quantitative measurements of the effects of two aspects of surface presentation of adhesion molecules, orientation and length, on their ligand binding two-dimensional affinity and kinetics, but also insights into the biophysical bases of such effects.

*Acknowledgments*—We thank Periasamy Selvaraj of Emory University School of Medicine for generous gifts of CD16A-transfected CHO cell and of mAbs of CLBFcgran-1 and X63, Charles Esmon of Oklahoma Medical Research Foundation for a generous gift of mAb 1478, and Kuo-Sen Huang of Hoffmann-La Roche Inc. for a generous gift of E-selectin construct ELE.

REFERENCES

1. Springer, T. A. (1994) *Cell* **76,** 301–314
2. Hynes, R. O. (2002) *Cell* **110,** 673–687
3. Vestweber, D., and Blanks, J. E. (1999) *Physiol. Rev.* **79,** 181–213
4. McEver, R. P. (2001) *Thromb. Haemost.* **86,** 746–756
5. McEver, R. P. (2002) *Curr. Opin. Cell Biol.* **14,** 581–586
6. van de Winkel, J. G., and Capel, P. J. (1993) *Immunol. Today* **14,** 215–221
7. Dustin, M. L., Bromley, S. K., Davis, M. M., and Zhu, C. (2001) *Annu. Rev. Cell Dev. Biol.* **17,** 133–157
8. Williams, T. E., Nagarajan, S., Selvaraj, P., and Zhu, C. (2001) *J. Biol. Chem.* **276,** 13283–13288
9. Chan, P. Y., and Springer, T. A. (1992) *Mol. Biol. Cell* **3,** 157–166
10. Patel, K. D., Nollert, M. U., and McEver, R. P. (1995) *J. Cell Biol.* **131,** 1893–1902
11. Yago, T., Leppänen, A., Qiu, H. Y., Marcus, W. D., Nollert, M. U., Zhu, C., Cummings, R. D., and McEver, R. P. (2002) *J. Cell Biol.* **158,** 787–799
12. Li, S. H., Burns, D. K., Rumberger, J. M., Presky, D. H., Wilkinson, V. L., Anostario, Jr. M., Wolitzky, B. A., Norton, C. R., Familletti, P. C., Kim, K. J., Goldstein, A. L., Cox, D. C., and Huang, K. S. (1994) *J. Biol. Chem.* **269,** 4431–4437
13. Chesla, S. E., Li, P., Nagarajan, S., Selvaraj, P., and Zhu, C. (2000) *J. Biol. Chem.* **275,** 10235–10246
14. Michael, K. E., Vernakar, V. N., Keselowsky, B. G., Meredith, J. C., Latour, R. A., and García, A. J. (2003) *Langmuir* **19,** 8033–8040
15. Dwir, O., Kansas, G. S., and Alon, R. (2000) *J. Biol. Chem.* **275,** 18682–18691
16. Geng, J. G., Bevilacqua, M. P., Moore, K. L., McIntyre, T. M., Prescott, S. M., Kim, J. M., Bliss, G. A., Zimmerman, G. A., and McEver, R. P. (1990) *Nature* **343,** 757–760
17. Erbe, D. V., Wolitzky, B. A., Presta, L. G., Norton, C. R., Ramos, R. J., Burns, D. K., Rumberger, J. M., Rao, B. N. N., Foxall, C., Brandley, B. K., and Lasky, L. A. (1992) *J. Cell Biol.* **119,** 215–227
18. Patel, K. D., Moore, K. L., Nollert, M. U., and McEver, R. P. (1995) *J. Clin. Investig.* **96,** 1887–1896
19. Moore, K. L., Patel, K. D., Bruehl, R. E., Li, F., Johnson, D. A., Lichenstein, H. S., Cummings, R. D., Bainton, D. F., and McEver, R. P. (1995) *J. Cell Biol.* **128,** 661–671
20. Nagarajan, S., Chesla, S. E., Cobern, L., Anderson, P., Zhu, C., and Selvaraj, P. (1995) *J. Biol. Chem.* **270,** 1–9
21. Ushiyama, S., Laue, T. M., Moore, K. L., Erickon, H. P., and McEver, R. P. (1993) *J. Biol. Chem.* **268,** 15229–15237
22. Mehta, P., Patel, K. D., Laue, T. M., Erickson, H. P., and McEver, R. P. (1997) *Blood* **90,** 2381–2389
23. Kofler, R., and Wick, G. (1977) *J. Immunol. Methods* **16,** 201–209
24. Chesla, S. E., Selvaraj, P., and Zhu, C. (1998) *Biophys. J.* **75,** 1553–1572
25. Williams, T. E., Selvaraj, P., and Zhu, C. (2000) *Biophys. J.* **79,** 1858–1866
26. Long, M., Zhao, H., Huang, K. S., and Zhu, C. (2001) *Ann. Biomed. Eng.* **29,** 935–946
27. Selvaraj, P., Plunkett, M. L., Dustin, M., Sanders, M. E., Shaw, S., and Springer, T. A. (1987) *Nature* **326,** 400–403
28. Piper, J. W., Swerlick, R. A., and Zhu, C. (1998) *Biophys. J.* **74,** 492–513
29. Scatchard, G. (1949) *Ann. N. Y. Acad. Sci.* **51,** 660–672
30. Zhu, C., and Williams, T. E. (2000) *Biophys. J.* **79,** 1850–1857
31. Mehta, P., Cummings, R. D., and McEver, R. P. (1998) *J. Biol. Chem.* **273,** 32506–32513
32. Keselowsky, B. G., Collard, D. M., and García, A. J. (2003) *J. Biomed. Mat. Res.* **66A,** 247–259
33. Takagi, J., Strokovich, K., Springer, T. A., and Walz, T. (2003) *EMBO J.* **22,** 4607–4615
34. Wong, J. Y., Kuhl, T. L., Israelachvili, J. N., Mullah, N., and Zalipsky, S. (1997) *Science* **275,** 820–822